Magnetic properties of Fe_1/Cr_N nanoinclusions in Fe

P.G. Alvarado-Leyva
Departamento de Física, Facultad de Ciencias, Universidad Autónoma de San Luis Potosí, Alvaro Obregon 64, 78000 San Luis Potosí, S.L.P., México

J.M. Montejano-Carrizales
Instituto de Física, "Manuel Sandoval Vallarta" , Universidad Autónoma de San Luis Potosí, Alvaro Obregon 64, 78000 San Luis Potosí, S.L.P., México

J.L. Morán-López
Instituto Potosino de Investigación Científica y Tecnológica, Apartado Postal 3-74 Tangamanga, 78231 San Luis Potosí, S.L.P., Mexico

Recibido el 11 de marzo de 2002; aceptado el 21 de agosto de 2002

The magnetic properties of Fe_1/Cr_N inclusions in a Fe matrix are calculated as a function of the Cr number of atoms N at zero temperature, and for $N \leq 168$. The electronic structure is determined by using a realistic *spd*-band Hamiltonian. The local magnetic moments $\mu(i)$ at the various cluster sites *i* are calculated selfconsistently in the unrestricted Hartree-Fock approximation. The results show clearly the importance of the local geometry and the magnetic interactions between neighbors. The matrix Fe atoms couple always antiferromagnetically to the Cr atoms, imposing for small N spin arrangements that overcome the antiferromagnetic interactions of the Cr cluster. The antiferromagnetic arrangement becomes possible in the interior of the cluster as the number of Cr atoms becomes larger than 88.

Keywords: Nanoinclusions; magnetic properties; magnetic local moments

Se calculan las propiedades magnéticas de inclusiones de Fe_1/Cr_N en una matriz de Fe, como una función del número N de átomos de Cr, a tempe ratura cero y valores de $N \leq 168$. La estructura electrónica se determina usando un hamiltoniano que toma en cuenta electrones de los tipos *s*, *p* y *d*. Usando la aproximación irrestricta de Hartree-Fock se calcula autoconsistentemente el momento magnético local $\mu(i)$ en los diferentes sit ios i del cúmulo. Los resultados muesran claramente la importancia de la ge ometría local y las interacciones magnéticas entre vecinos. Los átomos de Fe de la matriz se acoplan siempre antiferromagnéticamente a los átomos de Cr, imponiendo arreglos de espín que sobrepasan el antiferromagnetismo e ntre iones del cúmulo de Cr para valores pequeños de N. Los arreglos anti ferromagnéticos se presentan dentro del cúmulo de Cr cuando el número de 'atomos de Cr es mas grande que 88.

Descriptores: Inclusiones nanométricas; propiedades magnéticas; momentos locales magnéticos

PACS: 75.50.Rb

1. Introducción

The ability to produce experimentally systems with dimensions in the nanometer range and the unexpected properties observed, make nanoclusters a very attractive field of research. In particular magnetic nanostructures are expected to revolutionize the magnetic information industry [1].

Low dimensional systems involving Fe and Cr have been studied widely, mainly Fe/Cr/Fe(001) trilayers and Fe/Cr(001) multilayers because they exhibit interesting properties, like an oscillatory magnetic interlayer exchange coupling [2, 3], a giant magnetoresistance [4, 3], and short-period oscillatory exchange coupling [5]. Although throughout the last decade Fe/Cr/Fe(001) has served as a model system in the field of thin-film magnetism and by now it belongs to the most studied systems, both experimentally and theoretically, many questions are still open. An example is the dependence of the short-period oscillatory component of the exchange coupling with the structural properties of the interfaces in Fe/Cr/Fe(001) trilayers [6, 7].

Significant progress has been made in the understanding of the phenomena of exchange coupling between ferromagnetic layers separated by magnetic and non-magnetic layers. In part, this knowledge has been obtained by using Fe/Cr/Fe as a model system, in which, the structures produced experimentally [6, 7] can be closely approximated by the theoretical models [8–10]. This is important because of the big influence that the physical structure has on the magnetic properties. Nowadays, high quality Fe/Cr/Fe structures are possible because of the excellent Fe-Cr lattice match ($\simeq 0.6\%$).

Recently a number of important anomalies in the magnetic properties of the Fe/Cr and Fe/Cr/Fe systems have arisen, specifically with regard to the change in surface magnetization at low Cr coverage, the antiferromagnetic ordering between Cr layers, and the size of the Cr moment. Several experiments have detected these particular properties; scanning electron microscopy with polarization analysis (SEMPA) measurements [11], alternating gradient magnetometer measurements [12], polar Kerr measurements in Fe/Cr/Fe (001) [13], and Mössbauer spectroscopy [14]. On the other hand, several theoretical calculations exist in the scientific literature where these anomalies are predicted in low dimensional systems with Fe and Cr [8–10] and in Cr_N clusters embedded in bulk Fe [15].

There has been a great interest on studying how the interface will affect the properties of thin magnetic films, such as coercivity, magnetic domain structure, magnetization reversal and magnetoresistance [16–19]. These magnetic prop-

erties greatly affect the applications of thin magnetic films in the magnetic recording industry, as well as other applications in magnetoelectronics. So far, there are only a few theoretical examinations discussing the effects of surface/interface on magnetic films. This is probably due to the complicated nature of the problem. In addition to surface/interface effects many other factors, such as film thickness, composition, crystalline structure of the magnetic film, magnetic domain distribution and correlations contribute to the magnetic energy and determine the magnetization mechanism of a film. These are very important factors that cannot be neglected in practice. However, in order to distinguish which factor dominates, a more detailed study is necessary.

From a fundamental point of view, one of the most interesting features of such systems is the existence of strong long range interlayer magnetic coupling (IMC) between two successive ferromagnetic layers separated by nonmagnetic or antiferromagnetic spacers. These IMC were first observed by Grünberg *et al*. [2] and by Carbone and Alvarado [20] on Fe/Cr/Fe (001) sandwiches. They found that the interactions were antiferromagnetic (AF), that is, the magnetizations of two successive Fe layers were aligned antiparallel. Later on, in Fe/Cr (001) superlattices, these AF IMC, which have been observed for a wide range of Cr thickness, have been shown to be related to giant magnetoresistence [4] and explained by spin-dependent electron transport [21]. The different magnetoresistivities for the parallel/antiparallel configurations for adjacent magnetic layers was measured using differential microwave absorption method [22]. It was found that the IMC oscillates from AF to ferromagnetic (F) with the Cr thickness up to 50Å with a period of about 18Å (the magnetizations of two successive Fe layers alternate parallel/antiparallel) [3].

The aim of this paper is to study in detail the interdependence of the cluster inclusion and the magnetic interactions between Fe and Cr atoms. The geometrical structure consists of one Fe atom surrounded by N Cr-atoms ($N \leq 168$) located in *bcc* onion-like shells, and embedded in a Fe-bulk. The Cr-atoms are located as substitutional impurities. This specific problem has been chosen not only for its potential technological relevance, but for the rich magnetic behavior of Fe/Cr interfaces [23, 24].

In a previous paper [15] that deals with pure Cr_N clusters with $N \leq 51$, embedded in Fe, it was shown that the competition between the AF coupling in the Fe/Cr interface with the tendency to the antiferromagnetism of Cr offers a particularly interesting physical situation for studying the interplay between the magnetic properties of clusters and those of the environment. Moreover, the study of finite embedded clusters stresses the local aspects of the magnetic interactions between ferromagnetic and antiferromangetic materials. Here, we complement that study by analyzing the effect of a Fe atom in the center of the Cr cluster and report results for much larger clusters ($N \leq 168$). In this particular system, the magnetic behavior is not monotonic but changes as a function of the cluster size.

The rest of the paper is organized as follows. In Sec. 2 we present the details on how the electronic calculation was performed, which parameters were used and we give specific information on the geometry of the atomic inclusion. The results obtained are presented and discussed in Sec. 3. Finally, in Sec. 4 we present the conclusions of this work.

2. Model

2.1. Electronic part

Here, we calculate the ground state solution of the electronic structure. Due to the particular characteristic that magnetic transition metals present some properties that can be explained on the basis of localized models and others in the framework of itinerant models, the calculation of the finite temperature properties is still an unsolved problem.

The magnetic and electronic properties of transition metal clusters are determined by the 3*d* itinerant electrons, which are very sensitive to the local environment of the atoms. We consider a realistic model Hamiltonian for the valence *s*, *p* and *d* electrons, which includes intra-atomic Coulomb interactions in the unrestricted Hartee-Fock approximation. In the usual notation, the Hamiltonian is given by

$$H = \sum_{i\alpha\sigma} \varepsilon_{i\alpha\sigma} \hat{n}_{i\alpha\sigma} + \sum_{\alpha\beta\sigma} \sum_{i \neq j} t_{ij}^{\alpha\beta} \hat{c}_{i\alpha\sigma}^{\dagger} \hat{c}_{j\beta\sigma}, \qquad (1)$$

where *i* and *j* refer to the atomic sites, α and β to the orbitals ($\alpha, \beta \equiv s, p, d$), and σ to the spin. $\hat{c}_{i\alpha\sigma}^{\dagger}$ and $\hat{c}_{j\beta\sigma}$ are the creation and annihilation operators, respectively. The hopping integrals $t_{ij}^{\alpha\beta}$ are obtained from the canonical two-center approximation [25] and the environment dependent energy levels $\varepsilon_{i\alpha\sigma}$ are given by

$$\varepsilon_{i\alpha\sigma} = \varepsilon_{i\alpha}^{0} + \sum_{\beta} \left(U_{\alpha\beta} \Delta\nu_{i\beta} - \sigma \frac{J_{\alpha\beta}}{2} \mu_{i\beta} \right) + z_i \Omega_{\alpha}. \qquad (2)$$

The symbol $\varepsilon_{i\alpha}^{0}$ stands for the energy level of the orbital α of atom *i* in the paramagnetic solution of the bulk *e.g.*, Cr or Fe. The second term in Eq. (2) takes into account the level shifts due to the redistribution of the spin polarized electron density and to the resulting intra-atomic Coulomb interactions. $\Delta\nu_{i\beta} = \nu_{i\beta} - \nu_{i\beta}^{0}$, where $\nu_{i\beta} = \langle \hat{n}_{i\beta\uparrow} + \hat{n}_{i\beta\downarrow} \rangle$ is the average electronic occupation of the orbital $i\beta$ and $\nu_{i\beta\sigma}^{0}$ the corresponding average occupation in the bulk (paramagnetic solution). $\mu_{i\beta} = \langle \hat{n}_{i\beta\uparrow} - \hat{n}_{i\beta\downarrow} \rangle$ refers to the spin polarization of the orbital $i\beta$. The intra-atomic direct and exchange Coulomb integrals are denoted by $U_{\alpha\beta}$ and $J_{\alpha\beta}$, respectively. Finally, the last term in Eq. (2) takes into account the environment-dependent energy-level shifts due to non-orthogonality effects [25–27] and to the crystal-field potential of the neighboring atoms [28], which are approximately proportional to the local coordination number z_i. The average occupations $\nu_{i\alpha}$ and the local magnetic moments $\mu_{i\alpha}$ at site *i* are deter-

mined self-consistently by requiring

$$\langle \hat{n}_{i\alpha\sigma} \rangle = \int_{-\infty}^{\varepsilon_F} \rho_{i\alpha\sigma}(\varepsilon)\, d\varepsilon, \tag{3}$$

where $\rho_{i\alpha\sigma}(\varepsilon) = (-1/\pi)\mathrm{Im}\, G_{i\alpha\sigma,i\alpha\sigma}(\varepsilon)$ refers to the local density of states (DOS) of the spin-orbital $i\alpha\sigma$. In the case of finite embedded clusters, the Fermi energy ε_F is given by the matrix (in the present case Fe). Notice that charge transfers generally occurs between atoms and spin orbitals having different local environments. The local Green's functions $G_{i\alpha\sigma,i\alpha\sigma}(\varepsilon)$ are calculated from Eqs. (1) and (2) by using the recursion method [29]. The number of levels *M* of the continued fraction expansion of $G_{i\alpha\sigma,i\alpha\sigma}$ is chosen large enough so that the calculated orbital occupations and magnetic moments are independent of *M* (in practice we use $M = 15$–20). All the recursion coefficients are determined exactly without any spurious boundary effects. Therefore a large number of atoms (about 25 000–40 000) is involved in the real-space expansion.

2.2. Parameters

The parameters used in the calculations are determined as follows. The hopping integrals $t_{ij}^{\alpha\beta}$ between atoms of the same element are fitted to band-structure calculations for the pure elements [30, 31]. The heteroatomic hoppings at the cluster-matrix interface are obtained as the geometric average of the corresponding homoatomic hoppings. This has been proved to be a very good approximation in calculations for alloys and multilayers of transition metals [30, 32]. In the case of Fe and Cr, the *d*-electron exchange integrals are chosen to yield the proper magnetic moment and exchange splittings in the bulk at $T = 0$ [$J_{dd}(\mathrm{Fe}) = 1.05$ eV and $J_{dd}(\mathrm{Cr}) = 0.86$ eV]. Exchange integrals other than J_{dd} are neglected. For simplicity we ignore the differences between *s* and *p* Coulomb integrals (*i.e.*, $U_{ss} = U_{sp} = U_{pp}$ and $U_{sd} = U_{pd}$) and take the ratios between the direct Coulomb integrals $U_{ss} : U_{sd} : U_{dd}$ from atomic Hartee-Fock calculations [33].

2.3. Geometrical aspects

The systems studied here consist of a central site (denoted 0) and its neighbor shells, onion-like, around it in a *bcc* array. A shell is a set of atoms located at the same distance from the central site and with the same number type of neighbors. The lattice structure is illustrated in Fig. 1. Here the numbers label the atomic sites in the different shells *i*. The first shell (sites 1 in Fig. 1) contains the 8 first nearest neighbor (NN) atoms, located at the vertices of the cube. The next shell of neighbors (sites 2) has 6 atoms at a distance $1.15 d_{\mathrm{NN}}$ (d_{NN} is the nearest neighbor distance), and are located on the square face sites of the next generation cube. Shell 3 is formed by 12 atoms at a distance $1.52 d_{\mathrm{NN}}$ from the center, and so on.

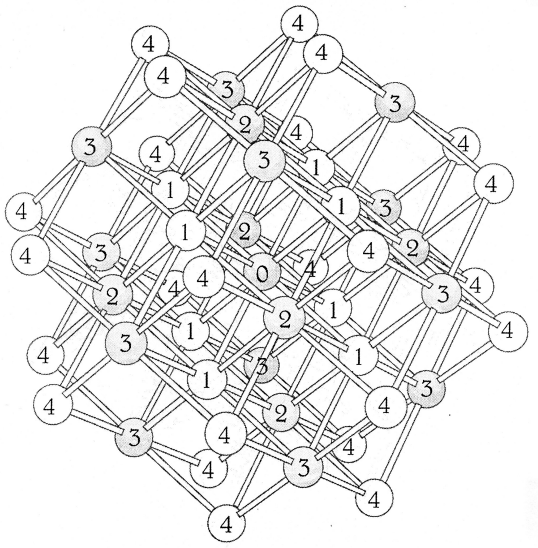

FIGURE 1. A cluster with 51 sites belonging to a *bcc* lattice. The numbers correspond to the nth neighbor shell to the central atom denoted by zero and the sites belonging to sublattice α (β) are shown as shaded (open) circles.

In Table I we list some of the geometrical characteristics of this *bcc* array up to the 20^{th} shell. In the first column we give the number of atoms in the shell. The shell numbers are given in the second column and first row. In the rest of the Table we give the number of first neighbors of an atom in i-shell located in j-shell. For example, an atom in shell 5 has 1 nearest neighbor in shell 1, 3 in shell 4, 3 in shell 7, and 1 in shell 10. Since we are dealing with a *bcc* lattice, the total number of NN must sum eight.

The shells are ordered as the radius increase. It is worth noticing that although shells 10 and 11 (and shells 14 and 15) are at the same distance they are considered as two different shells because their atoms have a different environment. This can be clearly seen in Table I.

In the present work the central site is a Fe-atom. The spacer between the central atom and the Fe-matrix (the bulk) is formed by Cr-shells. The number of shells depends on the total number of Cr-atoms. The Cr atoms are located as substitutional impurities in the Fe *bcc* lattice. Small strain effects resulting from the differences in the lattice constants are modeled by taking the nearest-neighbors distance d_{NN} at the cluster-matrix interface as the average between the NN distances of the pure elements. The electronic spin-density distribution is calculated self-consistently in each one of the non equivalent atomic sites.

It is important to note that in order to describe the antiferromagnetism in the Cr inclusion, it is necessary to subdivide the inclusion lattice sites into sublattices. Thus, the sites that belong to the sublattice β are those in shells 1, 4, 7, 10, 11, 13, 17, etc. and to the α sublattice are the sites in shells, 2, 3, 5, 6, 8, 9, 12, 14, 15, 16, etc. In Fig. 1 we show a cluster with 51 sites in which the sites belonging to sublattice α (β) are shown as shaded (open) circles.

TABLE I. The coordination numbers of an atom in shell i located in shell j, for the *bcc*-spherical arrangement.

		α	β	α	α	β	α	α	β	α	α	β	β	α	β	α	α	α	β	α	α	β
No. of shell																						
atoms	i	j	0	1	2	3	4	5	6	7	8	9	10	11	12	13	14	15	16	17	18	19	20
1	0		0	8																			
8	1		1	0	3	3	0	1															
6	2		0	4	0	0	4																
12	3		0	2	0	0	4	0	0	2													
24	4		0	0	1	2	0	1	1	0	2	1											
8	5		0	1	0	0	3	0	0	3	0	0	1										
6	6		0	0	0	0	4	0	0	0	0	0	0	4									
24	7		0	0	0	1	0	1	0	0	2	2	0	0	1	0	0	1					
24	8					2	0	0	2	0	0	0	2	0	2									
24	9					1	0	0	2	0	0	1	1	0	2	0	0	0	1				
8	10				1	0	0	0	3	0	0	0	0	0	0	3	0	0	0	1			
24	11				1	0	2	1	0	0	0	0	1	0	2	0	1						
12	12				2	0	0	0	0	0	4	0	0	0	0	0	0	0	0	2			
48	13				1	1	0	0	1	0	0	1	1	0	1	0	1	0					
6	14							4	0	0	0	0	0	0	0	0	0						
24	15				1	0	0	1	0	0	2	0	0	0	2								1
24	16							2	0	2	0	0	0	0	0	0	0	0	0	0	0		
24	17					1	0	0	0	0	0	2	0	0	1	1	0						
24	18							1	0	2	0	0	0	1	0	0	0						
8	19					1	0	0	0	0	0	0	3	0	0	0	0						
24	20							1	0	0	1	0	0	0	0								
24	21								1	0	2	0	1	0	0								
24	22							2	0	0	0	0	0	0	2								
48	23							1	0	0	0	1	0	0	1								
24	24								0	1	0	0	0	1	0								
48	25									0	1	0	1	0	0								

3. Results and discussion

In all the cases studied local charge neutrality is imposed at each site *i*, *i.e.*, $\Delta\nu_{i\beta} = 0$ [30]. The self-consistent calculations involved the central Fe atom, all the Cr cluster atoms and the Fe-matrix atoms at least up to the fifth shell away from the interface between the cluster and the matrix atoms. Beyond this shell the spin-density distribution is taken to be the same as in pure Fe. Due to the characteristics of the system studied here, there are two interfaces: one between the Fe-central site and the Cr-atoms of the spacer and the other between the boundary atoms of the Cr inclusion and the Fe-matrix. As it can be seen from Table I, the central site only coordinates with the 8 Cr-atoms of the first shell, then this interface is the same for any value of $N \geq 8$. On the other hand the interface between the cluster inclusion and the Fe matrix becomes more complex as the number of Cr-atoms increases. In addition, the fact that the Cr lattice consists of two sublattices, makes the interface unique of each cluster. For example, for $N = 8$ the interface is between the 8 Cr-atoms in shell 1 (a cube of length size $\sqrt{2}d_{\rm NN}$, see Fig. 1) and the 26 Fe-atoms (a cube of length size $2\sqrt{2}d_{\rm NN}$) in shells 2, 3, and 5 (see Table I). For $N = 14$, the interface is between the 14 Cr-atoms in shells 1 and 2 (a cube of Cr-atoms with one atom over each face) and the 44 Fe-atoms in the shells 3, 4, and 5 (a cube with 4 atoms over each face). For $N = 26$ the interface is between the 26 Cr-atoms in shells 1, 2 and 3, and the 56 Fe atoms in shells 4, 5, and 7. The interfaces of the cluster with $N = 14$ and 26 have the geometrical shape of a cube without the corner sites.

Starting with $N = 50$ some Cr shells are totally surrounded by Cr atoms; the 6 Cr-atoms in shell 2 have that property; the same occurs for the 18 Cr-atoms in shells 2 and 3 for $N = 88$. One has to notice further that the sites in shells 2 and 3 belong to the same sublattice β and are not nearest neighbors. Similarly the 50 atoms in shells 2,3,4, and 5 in the $N = 144$ inclusion form a compact core of Cr atoms surrounded only by Cr-atoms.

Taking into account all the various non-equivalent sites in the cluster, we calculated selfconsistently the electronic local density of states (LDOS). In Fig. 2 we show the results for some particular cases that illustrate the hybridization between the Fe and Cr electrons. In the upper panel we show the LDOS for bulk Fe (thick line), and the LDOS for the Fe central atom for $N = 8$ thin broken line) and 136 (thin solid line). We notice that the LDOS for the $N = 8$ cluster differs considerably from the bulk spectrum. In the down spin density of states there are various peaks produced by the interaction with the *d* electrons of the 8 surrounding Cr atoms. As a result, the magnetic moment of the central Fe results negative. When the number of Cr atoms increases to 136, the LDOS gets smoother but the number of down electrons is also larger than the up electrons, producing a negative magnetic moment. In the lower panel we show the bulk Cr LDOS (thick solid line), and the average density of states of the Cr atoms surrounding the Fe atom and embedded in the Fe matrix, for the two cluster sizes. Most of the Cr atoms are located at the boundary and the electronic spectra is strongly influenced by the Fe atoms. In all the cases the magnetic moment of these atoms are large and negative.

The results are better understood in terms of the local magnetic moments. In Table II we present the results for the various cases studied here. For each cluster there are three rows, in the first row we give the kind of atoms in each shell, Fe or Cr, in the second row the value of the magnetic moment $\mu(i)$ of atoms in sites of shell i, and in the third row the number of NN-Cr(Fe)-atoms to Fe(Cr) in shell i. We recall that the total number of NN is eight. The various cluster sizes were obtained by adding a full shell of Cr atoms to the

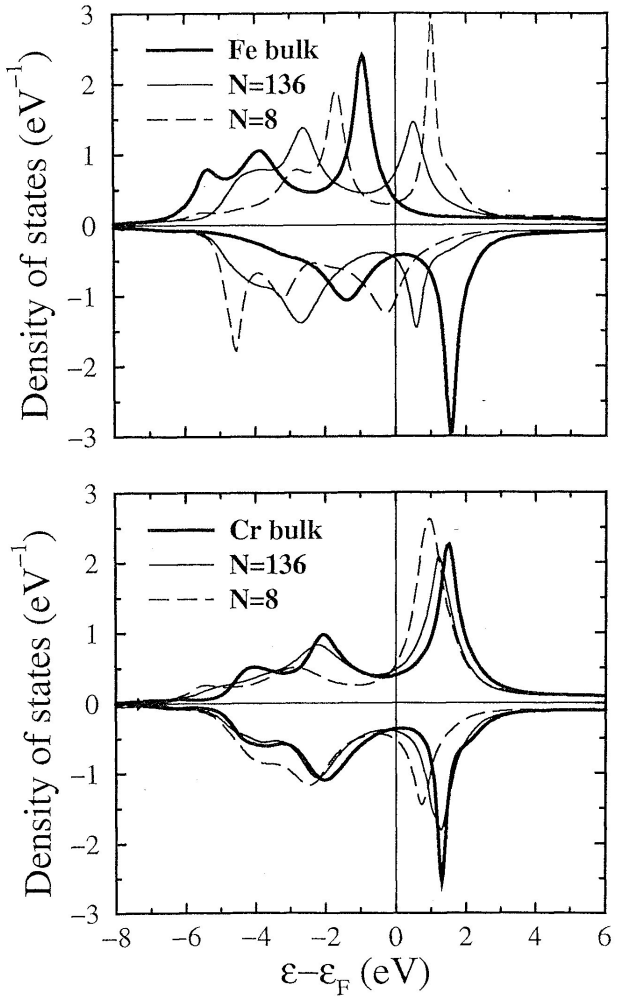

FIGURE 2. The electronic local density of states (LDOS) for some particular cases. In the upper panel the LDOS for bulk Fe (thick line), and the corresponding to the Fe central atom for $N = 8$ (thin broken line) and 136 (thin solid line). In the lower panel the bulk Cr LDOS (thick solid line), and the average density of states of the Cr atoms surrounding the Fe atom and embedded in the Fe matrix, for the two cluster sizes.

previous cluster. The largest cluster consists of the central Fe atom surrounded by the 11 Cr neighbor shells. To understand the results is important to notice that the Cr piece of lattice has to be subdivided into two sublattices. Assuming that the Fe central atom is in an α-site, the shells that belong to the same sublattice are 2, 3, 5, 6, 8, and 9. On the other hand, the shells 1, 4, 7, 10, and 11 belong to the β sublattice.

In Table II we see how the selfconsistent solution for the magnetic moments at the various non equivalent sites change as a function of N. We notice that the sign of the interactions as well as the magnitude of the local moments depend strongly on the size of the inclusion. This reflects the high dependence of the solutions on the geometrical environment.

With the aid of Tables I and II we build Table III, which contains the type of interaction (antiferromagnetic AF or ferromagnetic F) between the atoms in shell i with their nearest neighbor atoms in shells j. The information on the sublattice type in the Cr inclusion is also included. We present the results for $N = 26, 136$, and 168. If the magnetic interactions would follow the bulk behavior, one would expect an arrangement in which the central Fe atom is coupled AF with the first shell of Cr atoms, the Cr atoms would couple AF among themselves and the Cr atoms at the boundary of the inclusion would couple AF with the Fe matrix. Since the tables are symmetric with respect to the diagonal and the F-order in the Fe-matrix is unchanged, the tables contain only the shells to which the boundary Cr atoms are connected to the Fe matrix. The vertical heavy line marks the boundary between the inclusion and the matrix. To illustrate the information contained in the tables, in the case of $N = 26$, the Cr atoms in the third shell (the most external Cr atoms) couple AF the Cr atoms in the first shell and also AF with the Fe-matrix atoms in shells 4 and 7.

One can observe that the AF interaction between the Fe matrix and the Cr atoms at the boundary, rules the magnetic arrangement of the cluster. Due to the geometry of the *bcc* lattice there is frustration and not all the boundary atoms can fulfill an AF arrangement. The cases in which there are no frustration bonds in the cluster boundary are those for $N = 8, 14, 64, 160$, and 168. However, it is interesting that in the first case the coupling among the eight Cr atoms and the central Fe atom is ferromagnetic. The other cases, $N = 64$ and 168 present a large number of frustrated bonds in the Cr cluster; *i.e.* the interaction between themselves is F.

The cases $N = 26$ and 50 are the ones with less frustrations in the whole system. The only frustration in the first (second) case is between the Cr atoms in the first (third) shell with the Fe atoms in the fifth (seventh) shell. The cases with the largest number of frustrated bonds are $N = 64$ and 168, where the Cr atoms in the fifth and tenth shells couple ferromagneticaly with other Cr atoms within the cluster, respectively.

In relation with the magnitude of the local magnetic moments we can notice the following trends. a) One can notice that in cases with a large number of frustrated bonds, the selfconsistent solutions yield very small values for the magnetic moments. One can notice that $\mu(i) \sim 0$ for Cr-sites that coordinates to more than two frustrated sites. For example $\mu(3)$ for $N = 58$ and $\mu(2)$ for $N = 64$. b) On the other hand, in situations where the number of frustrated bonds is small, the magnetic moments $\mu(i)$ in sites occupied by Cr-atoms that coordinate only with Cr-atoms is close to the magnetic moment of the bulk for Cr. Examples are $\mu(2)$ for $N = 50$ and $\mu(2)$ and $\mu(3)$ for $N = 88$. c) The value of the magnetic moments of the Cr atoms $|\mu(i)|$ is enhanced ($|\mu(i)| > \mu_b$) for sites that coordinate with four or more Fe-atoms without frustration; for example $\mu(2)$ and $\mu(3)$ for $N = 26$, $\mu(4)$ for $N = 50$ and $\mu(7)$ for $N = 88$. D) With respect to the Fe atoms at the boundary, the value of the magnetic moment of Fe in sites that coordinate with Cr-atoms is smaller than the value in bulk Fe. As the Cr-coordination increases, the value of $\mu(i)$ decreases from 2.24 to 1.68.

TABLE II. The occupation (Cr or Fe) of the sites at the various shells i, the local magnetic moments $\mu(i)$ (in units of μ_B), and the type of neighbor for the various cases in the system *bcc* $Fe_1/Cr_N/Fe_\infty$. The lattice structure and the labels i for the different atomic sites are shown in Fig. 1.

N	i	0	1	2	3	4	5	6	7	8	9	10	11	12	13	14	15	16	17	18	19	20	21
		Fe	Cr	Fe	Fe	Fe	Fe	Fe	Fe														
8		−1.28	−1.79	1.79	2.05	2.27	2.17	2.24	2.27														
		8Cr	8Fe	4Cr	2Cr	8Fe	1Cr	8Fe	8Fe														
		Fe	Cr	Cr	Fe	Fe	Fe	Fe	Fe														
14		−1.05	−0.77	−0.50	2.00	2.14	2.16	2.22	2.27														
		8Cr	5Fe	4Fe	2Cr	1Cr	1Cr	8Fe	8Fe														
		Fe	Cr	Cr	Cr	Fe	Fe	Fe	Fe	Fe	Fe												
26		−0.20	0.56	−1.11	−1.56	1.90	2.05	2.26	2.15	2.27	2.27												
		8Cr	2Fe	4Fe	6Fe	3Cr	1Cr	8Fe	1Cr	8Fe	8Fe												
		Fe	Cr	Cr	Cr	Cr	Fe	Fe	Fe	Fe	Fe	Fe	Fe										
50		0.34	−0.50	0.49	0.24	−1.21	1.68	1.70	2.12	1.99	2.14	2.29	2.27										
		8Cr	2Fe	8Cr	2Fe	5Fe	4Cr	4Cr	1Cr	2Cr	1Cr	8Fe	8Fe										
		Fe	Cr	Cr	Cr	Cr	Cr	Fe	Fe	Fe	Fe	Fe	Fe	Fe									
58		0.35	−0.22	0.28	0.02	−0.84	−0.42	1.77	1.98	2.01	2.13	2.17	2.26	2.27									
		8Cr	1Fe	8Cr	2Fe	4Fe	4Fe	4Cr	2Cr	2Cr	1Cr	1Cr	8Fe	8Fe									
		Fe	Cr	Cr	Cr	Cr	Cr	Cr	Fe	Fe	Fe	Fe	Fe	Fe	Fe								
64		0.11	0.05	−0.004	−0.21	−0.41	−0.73	−0.89	1.97	1.97	2.13	2.18	2.13	2.28	2.27								
		8Cr	1Fe	8Cr	2Fe	3Fe	4Fe	4Fe	2Cr	2Cr	1Cr	1Cr	1Cr	8Fe	8Fe								
		Fe	Cr	Cr	Cr	Cr	Cr	Cr	Cr	Fe	Fe	Fe	Fe	Fe	Fe	Fe	Fe	Fe	Fe				
88		0.17	−0.52	0.50	0.55	−0.75	0.45	−0.35	−1.41	1.74	1.89	2.09	2.19	2.06	2.28	2.24	2.16	2.26	2.30				
		8Cr	1Fe	8Cr	8Cr	3Fe	1Fe	4Fe	6Fe	4Cr	3Cr	1Cr	1Cr	2Cr	8Fe	8Fe	1Cr	8Fe	8Fe				
		Fe	Cr	Cr	Cr	Cr	Cr	Cr	Cr	Cr	Fe	Fe	Fe	Fe	Fe	Fe	Fe	Fe	Fe				
112		−0.02	0.07	−0.04	−0.09	0.02	−0.08	−0.71	−0.54	−0.68	1.80	2.06	1.89	1.98	2.14	2.26	2.16	2.26	2.28				
		8Cr	1Fe	8Cr	8Cr	1Fe	1Fe	4Fe	4Fe	4Fe	3Cr	1Cr	3Cr	2Cr	1Cr	8Fe	1Cr	8Fe	8Fe				
		Fe	Cr	Cr	Cr	Cr	Cr	Cr	Cr	Cr	Cr	Fe	Fe	Fe	Fe	Fe	Fe	Fe	Fe	Fe	Fe		
136		−0.196	0.45	−0.45	−0.45	0.49	−0.47	−0.91	0.23	−0.98	−1.20	1.67	1.75	2.00	2.01	2.32	2.12	2.28	2.16	2.26	2.29		
		8Cr	1Fe	8Cr	8Cr	8Cr	1Fe	4Fe	2Fe	4Fe	5Fe	4Cr	4Cr	2Cr	2Cr	8Fe	1Cr	8Fe	1Cr	8Fe	8Fe		
		Fe	Cr	Cr	Cr	Cr	Cr	Cr	Cr	Cr	Cr	Cr	Fe	Fe	Fe	Fe	Fe	Fe	Fe	Fe	Fe	Fe	Fe
144		−0.18	0.37	−0.38	−0.36	0.41	−0.31	−0.87	0.12	−0.91	−0.88	−0.39	1.75	1.97	2.10	2.31	1.97	2.28	2.12	2.26	2.16	2.25	2.27
		8Cr	1Fe	8Cr	8Cr	8Cr	8Cr	4Fe	2Fe	4Fe	4Fe	4Fe	4Cr	2Cr	2Cr	8Fe	2Cr	8Fe	1Cr	8Fe	1Cr	8Fe	8Fe
		Fe	Cr	Cr	Cr	Cr	Cr	Cr	Cr	Cr	Cr	Fe	Cr	Fe	Fe	Fe	Fe	Fe	Fe	Fe	Fe		
160		−0.02	0.05	−0.004	−0.03	0.02	−0.09	0.09	−0.18	−0.25	−0.64	1.64	−0.69	1.96	1.96	1.74	2.10	2.00	2.15	2.13	2.29		
		8Cr	1Fe	8Cr	8Cr	8Cr	1Fe	8Cr	2Fe	2Fe	4Fe	4Cr	4Fe	2Cr	2Cr	4Cr	1Cr	2Cr	1Cr	8Fe	8Fe		
		Fe	Cr	Cr	Cr	Cr	Cr	Cr	Cr	Cr	Cr	Cr	Cr	Fe	Fe	Fe	Fe	Fe	Fe	Fe	Fe	Fe	Fe
168		0.01	−0.09	0.12	−0.12	−0.11	0.11	0.20	−0.32	−0.10	−0.31	−0.82	−0.83	1.95	1.96	1.72	1.96	2.01	2.12	2.12	2.16	2.25	2.28
		8Cr	1Fe	8Cr	8Cr	8Cr	8Cr	8Cr	2Fe	2Fe	3Fe	4Fe	4Fe	2Cr	2Cr	4Cr	2Cr	2Cr	1Cr	1Cr	1Cr	8Fe	8Fe

TABLE III. The interaction between the sites in shell i with sites in shell j (A antiferromagnetic and F ferromagnetic), for the various cases in the system *bcc* $Fe_1/Cr_N/Fe_\infty$; $N = 26$, 136 and 168. Numbers in boldface mean that the magnetic moment is very small.

								$N = 26$												
			β	α	β	β	α	β	β	α										
i	j	0	1	2	3	4	5	6	7											
β	0		AF																	
α	1	AF		AF	AF		F													
β	2		AF			AF														
β	3		AF			AF			AF											
								$N = 136$												
			β	α	β	β	α	β	β	α	β	β	α	α	β	α	β	β	β	α
i	j	0	1	2	3	4	5	6	7	8	9	10	11	12	13	14	15	16	17	
β	0		AF																	
α	1	AF		AF	AF		AF													
β	2		AF			AF														
β	3		AF			AF			AF											
α	4			AF	AF		AF	AF		AF	AF									
β	5		AF			AF			AF			AF								
β	6					AF							AF							
α	7				AF		AF			AF	AF			F			F			
β	8					AF			AF				AF		AF					
β	9					AF			AF			AF	AF		AF					AF
								$N = 168$												
			β	α	β	β	α	β	β	α	β	β	α	α	β	α	β	β	β	α
i	j	0	1	2	3	4	5	6	7	8	9	10	11	12	13	14	15	16	17	
β	**0**		AF																	
α	1	AF		AF	F		AF													
β	2		AF			AF														
β	3		F			F			F											
α	4			AF	F		AF	AF		F	F									
β	5		AF			AF			AF			AF								
β	6					AF							AF							
α	7				F		AF			F	F			AF			AF			
β	8					F			F				F		AF					
β	9					F			F			F	F		AF					AF
α	10						AF				F						AF			
α	11							AF		F	F					AF		AF		

In the case Fe_1Cr_8, the Fe $|\mu(0)|$ is remarkably decreased as compared to the magnetization of bulk Fe ($\mu_b = 2.2\mu_B$); this change in the modulus is approximately 42%. Moreover one notices that the Fe moment is parallel to the Cr shell ($i = 1$) and antiparallel with the Fe-matrix ($i \geq 3$). Furthermore, the magnetic moment of the Cr atoms $\mu(1)$ is remarkably enhanced as compared to the bulk value $\mu_b = |0.6\mu_B|$ and it is antiparallel to the Fe matrix. Similar trends hold for larger Cr_N spacers, and for Fe/Cr multilayers [32, 24, 34]. The antiparallel alignment at the interface spacer-matrix was explained in terms of the hybridizations between Fe and Cr *d* orbitals [8, 15]. The hibridizations between Fe and Cr *d* orbitals at the interface tend to shift the majority (up) *d* levels of Fe to higher energies and the minority (down) Fe *d* levels to lower energies. This reduces the energy and stabilizes the ferromagnetic solution [8]. The value of $\mu(3)$ is decreased approximately 18.4%, because these sites have 4 Cr NN and 4 Fe NN whose moments point in opposite directions (see Table II and Fig. 1).

A much more interesting behavior is found as the thickness of the Cr spacer increases. For $N = 14$ there are two Cr-shells and both form the interface with the Fe matrix. Here, the AF coupling between Cr sites and Fe matrix dominates but the magnetic behavior of the Cr atoms is ferromagnetic-like. Furthermore, there is an antiparallel alignment between the central Fe atom and the first shell of atoms in the Fe-matrix. In the cluster with $N = 26$, one of the cases that present less frustrations, appears the typical antiparallel (AF) alignment between the Fe atom and Cr elements, and into the Cr spacer, but still exists the AF coupling between the Fe central atom and the first shell of the Fe-matrix (see Table III).

For $N = 50$, the other case with less frustrations, there is a transition in the alignment between the central Fe atom and the Fe-matrix. The alignment is parallel, but $\mu(0)$ is remarkably decreased with respect to the Fe bulk magnetization. This reduction can be explained in terms of the smaller exchange splitting at the Cr atoms surrounding the Fe atom. In the Cr spacer there are magnetic mismatches; the type 3 site has a reduced magnetic moment because this site is at the interface and has NN Cr-atoms in the first and in the fourth shells. The magnetic coupling between $\mu(3)$ with his NN shells is AF-like but with his Fe NN shell is ordered ferromagnetically. This mismatch produces the small value of $\mu(3)$.

A similar behavior is found in Cr_{58}. $\mu(3)$ is almost 0, because the interface prefers the AF coupling with the matrix but a perfect AF coupling into the spacer is not possible. This magnetic frustration is reflected in the small values of $\mu(1)$ and $\mu(2)$. Similar results were found in other Fe/Cr structures [9].

The strongest effect of the magnetic frustrations at the interface is found in Cr_{64}. In this case the Cr shells, 3, 4, 5 and 6 are located at the interface, and prefers the AF order with the Fe-matrix but F coupling between themselves, see Table III, therefore $\mu(1)$ and $\mu(2)$ are strongly reduced (see Table II). The magnetic moment $\mu(2)$ is almost 0. The parallel alignment between the Fe elements is unchanged and $\mu(0)$ acquires the lowest value for all the cases. This type of results were also found in Fe/Cr multilayers [10]. Notice that the $\mu(i)$ of Fe atoms close to Cr_N are slightly reduced. A similar behavior is found for atoms close to Cr atomic impurities [35] or at the interface of Fe/Cr overlayers [8] and

multilayers [34]. This can be qualitatively understood as the result of hybridizations between majority (minority) Fe *d* orbitals and the corresponding minority (majority) *d* orbitals of Cr, which increase the effective local *d*-band width at the Fe atoms of the interface.

Finally, we show in Fig. 3 the self-consistent solution of the magnetic moment of the Fe central atom as a function of chromium atoms in the cluster. As mentioned above the magnetic moment of the Fe matrix atoms are imposed positive. Thus, this figure illustrates, at a small scale, the oscillatory behavior of the magnetic coupling among Fe atoms separated by Cr atoms.

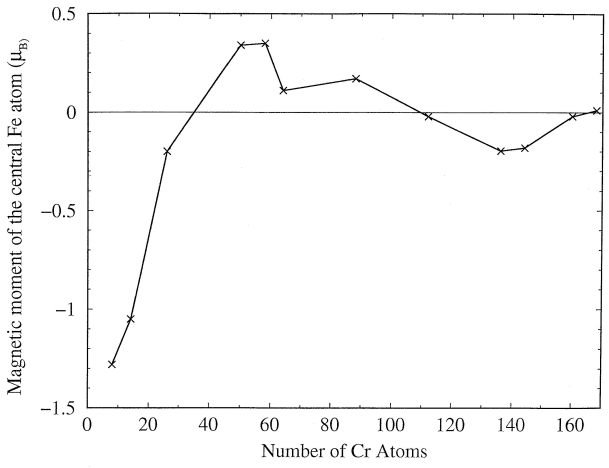

FIGURE 3. The self-consistent solution of the magnetic moment of the Fe central atom as a function of chromium atoms in the cluster.

4. Conclusions

The interface effects on the magnetic moments in the system $Fe_1/Cr_N/Fe_\infty$ have been determined by solving a realistic *spd*-band model Hamiltonian in the unrestricted Hartree-Fock approximation. The competition between the ferromagnetic order of the matrix and the tendency of Cr to antiferromagnetic-like order results in a remarkable dependence of the magnetic solutions on size and environment. The main conclusions are summarized as follows.

a) The magnetic coupling between the Cr boundary atoms and the Fe matrix is always antiferromagnetic, the $\mu(i)$ of Cr atoms are enhanced considerably by the presence of Fe atoms in their NN shell [*e.g.*, $\mu(2) = -1.79\mu_B$ in Cr_8 and $\mu(3) = -1.56\mu_B$ in Cr_{26}]. On the other hand, the $\mu(i)$ Fe atoms close to the cluster usually tend to be reduced, and the ferromagnetic order of the boundary Fe atoms of the matrix is never altered by the cluster atoms.

b) The magnetic coupling between the central Fe atom and its first Cr NN shell is ferromagnetic for Cr_8, Cr_{14} and Cr_{64} and antiferromagnetic for the other cases studied here. The value of the magnetic moment of the central Fe atom $\mu(0)$ increases for $N = 8$ to 26 and changes sign for $N = 50$, *i.e.*, exists a transition in the alignment between the Fe atom and the Fe-matrix. The alignment is first antiparallel, then it turns parallel, and changes sign again at $N = 112$. Similar oscillatory behavior as a function of the Cr spacer thickness was observed first in thin films [3, 24] .

c) In the Cr cluster, the magnetic order is very complex: for Cr_{14} it is F order, for $N = 26$ and 50 it is AF order and for $N \geq 58$ the AF and F order coexist. Magnetic frustrations are present when the AF order within the cluster shells is not compatible with the antiparallel alignment of the NN moments at the interface. These frustrations lead to a small values of $\mu(i)$ in the cluster [*e.g.*, $\mu(3) = 0.02\mu_B$ in Cr_{58}; $\mu(1) = 0.05\mu_B$ and $\mu(2) = -0.004\mu_B$ in Cr_{64}].

d) The self-consistent solution of the magnetic moment of the Fe central atom as a function of chromium atoms shows: i) the oscillatory coupling among this atom and the matrix Fe atoms and ii) a reduction in magnitude. This last fact is in accordance to the reduced value of the magnetic moment of Fe observed in neutron scattering experiments in diluted FeCr alloys [36].

Acknowledgements

This work was done under the auspices of CONACyT (Mexico) through grants G-25851-E and W-8001 (Millennium Initiative). One of the authors (P.G.A.L.) acknowledges to FAI-UASLP (Mexico) under contract C00-FAI-11-13.76.

1. *Magnetic Nanostructures*, edited by H. Singh Nalwa (American Scientific Publishers, California, 2002)
2. P. Grünberg *et al.*, *Phys. Rev. Lett.* **57** (1986) 2442.
3. S.S.P. Parkin, N. More, and K.P. Roche, *Phys. Rev. Lett.* **64** (1990) 2304.
4. M.N. Baibich *et al.*, *Phys. Rev. Lett.* **61** (1988) 2472; R. Schad *et al.*, *Phys. Rev. B.* **59** (1999) 1242; R. Schad *et al.*, *J. Magn. Magn. Mater.* **198** (1999) 104.
5. J. Unguris, R.J. Celotta, and D.T. Pierce, *Phys. Rev. Lett.* **67** (1991) 140.
6. C.M. Schmidt *et al.*, *Phys. Rev. B* **60** (1999) 4158; G. Palasantzsas, *J. Appl. Phys.* **86** (1999) 6879.
7. A. Moschel, R.A. Hyman, A. Zangwill, and M.D. Stiles, *Phys. Rev. Lett.* **77** (1996) 3653.
8. S. Mirbt, O. Ericksson, B. Johansson, and H.L. Skriver, *Phys.*

Rev. B **52** (1995) 15070; S. Mirbt, I.A. Abrikosov, B. Johansson, and H.L. Skriver, *ibid* **55** (1997) 67.

9. D. Stoeffler and F. Gautier, *J. Magn. Magn. Mater.* **147** (1995) 260.
10. Jian-hua Xu and A.J. Freeman, *Phys. Rev. B* **47** (1993) 165.
11. D.T. Pierce, R.J. Celotta, and J. Unguris, *J. Appl. Phys.* **73** (1993) 6201; J. Unguris, R.J. Celotta, and D.T. Pierce, *Phys. Rev. Lett.* **69**, (1992) 1125.
12. C. Turtur and G. Bayreuther, *Phys. Rev. Lett.* **72** (1994) 1557.
13. A.J. Ives, J.A.C. Bland, R.J. Hicken, and C. Daboo, *Phys. Rev. B* **55** (1997) 12428.
14. K. Mibu *et al.*, *Phys. Rev. Lett.* **84** (2000) 2243.
15. P. Alvarado, J. Dorantes-Dávila, and G.M. Pastor, *Phys. Rev. B* **58** (1998) 12216.
16. *Ultrathin Magnetic Structures I and II*, edited by J.A.C. Bland and B. Heinrich (Springer, New York, 1994).
17. C.H. Chang and M.H. Kryder, *J. Appl. Phys.* **75** (1994) 6864.
18. P. Bruno *et al.*, *J. Appl. Phys.* **68** (1990) 5759.
19. J. Barnas and G. Palasantzsas, *J. Appl. Phys.* **82** (1997) 3950.
20. C. Carbone and S.F. Alvarado, *Phys. Rev. B* **36** (1987) 2433.
21. R.Q. Hood, L.M. Falicov, and D.R. Penn, *Phys. Rev. B* **49** (1994) 368; Y. Asano, A. Oguria, and S. Maekawa, *ibid* **48** (1993) 6192; J. Barnas and Y. Bruynseraede, *ibid* **53** (1996) 5449.
22. Z. Frait *et al.*, *Solid State Commun.* **112** (1999) 569.
23. T.S. Toellner *et al.*, *Phys. Rev. Lett.* **74** (1995) 3475; E.E. Fullerton *et al.*, *ibid* **75** (1995) 330.
24. A. Azevedo *et al.*, *Phys. Rev. Lett.* **76** (1996) 4837.
25. W.A. Harrison, *Electronic Structure and Properties of Solids* (Freeman, San Francisco, 1980).
26. J. Dorantes-Dávila, A. Vega, and G.M. Pastor, *Phys. Rev. B* **47** (1993) 12995; J. Dorantes-Dávila and G.M. Pastor, *ibid* **51** (1995) 16627.
27. M. van Schilfgaarde and W.A. Harrison. *Phys. Rev. B* **33** (1986) 2653.
28. G.M. Pastor, J. Dorantes-Dávila, and K.H. Bennemann, *Chem. Phys. Lett.* **148**, (1988) 459.
29. R. Haydock, in *Solid State Physics*, edited by H. Ehrenreich, F. Seitz, and D. Turnbull (Academic, New York, 1980), Vol 35, p. 215.
30. R.H. Victora, L.M. Falicov, and S. Ishida, *Phys. Rev. B* **30** (1984) 3896.
31. D.A. Papaconstantopoulos, *Handbook of the Band Structure of Elemental Solids* (Plenum, New York, 1986).
32. M. Freyss, D. Stoeffler, and H. Dreyssé. *Phys. Rev. B* **56** (1997) 6047.
33. J.B. Mann, Los Alamos Science Laboratory Report No. LA-3690, 1967 (unpublished).
34. K. Ounadjela *et al.*, *Europhys. Lett.* **15** (1991) 875.
35. B. Drittler *et al.*, *Phys. Rev. B* **40** (1989) 8203.
36. M.F. Collins and G.G. Low, *Proc. Phys. Soc. London* **86** (1965) 535; A.T. Aldred, B.D. Rainford, J.S. Kouvel, and T.J. Hicks, *Phys. Rev. B* **14** (1976) 228.